Molecular examination of bone marrow stromal cells and chondroitinase ABC-assisted acellular nerve allograft for peripheral nerve regeneration

YING WANG[1*], HUA JIA[2*], WEN-YUAN LI[1], LI-XIN GUAN[1], LINGXIAO DENG[3],
YAN-CUI LIU[1] and GUI-BO LIU[1]

[1]Department of Anatomy, Mudanjiang College of Medicine, Mudanjiang, Heilongjiang 157011;
[2]Department of Anatomy, College of Basic Medical Sciences, Ningxia Medical University,
Yinchuan, Ningxia Hui 750004, P.R. China; [3]Department of Anatomy and Cell Biology,
Indiana University School of Medicine, Indianapolis, IN 46202, USA

Abstract. The present study aimed to evaluate the molecular mechanisms underlying combinatorial bone marrow stromal cell (BMSC) transplantation and chondroitinase ABC (Ch-ABC) therapy in a model of acellular nerve allograft (ANA) repair of the sciatic nerve gap in rats. Sprague Dawley rats (n=24) were used as nerve donors and Wistar rats (n=48) were randomly divided into the following groups: Group I, Dulbecco's modified Eagle's medium (DMEM) control group (ANA treated with DMEM only); Group II, Ch-ABC group (ANA treated with Ch-ABC only); Group III, BMSC group (ANA seeded with BMSCs only); Group IV, Ch-ABC + BMSCs group (Ch-ABC treated ANA then seeded with BMSCs). After 8 weeks, the expression of nerve growth factor, brain-derived neurotrophic factor and vascular endothelial growth factor in the regenerated tissues were detected by reverse transcription-quantitative polymerase chain reaction and immunohistochemistry. Axonal regeneration, motor neuron protection and functional recovery were examined by immunohistochemistry, horseradish peroxidase retrograde neural tracing and electrophysiological and tibialis anterior muscle recovery analyses. It was observed that combination

Correspondence to: Dr Ying Wang, Department of Anatomy, Mudanjiang College of Medicine, 3 Tongxiang Street, Mudanjiang, Heilongjiang 157011, P.R. China
E-mail: yingwangphd@yahoo.com

*Contributed equally

therapy enhances the growth response of the donor nerve locally as well as distally, at the level of the spinal cord motoneuron and the target muscle organ. This phenomenon is likely due to the propagation of retrograde and anterograde transport of growth signals sourced from the graft site. Collectively, growth improvement on the donor nerve, target muscle and motoneuron ultimately contribute to efficacious axonal regeneration and functional recovery. Thorough investigation of molecular peripheral nerve injury combinatorial strategies are required for the optimization of efficacious therapy and full functional recovery following ANA.

Introduction

Despite several decades of research, peripheral nerve injury (PNI) repair remains suboptimal, as full recovery is difficult to achieve (1). Nerve autografting remains the gold standard in PNI therapy (2); however, autografting may be a clinical challenge due to the creation of a secondary injury site and the limited availability of donor graft resources. Peripheral nerve allografts have proved efficacious in the treatment of nerve injury, and thus provide a viable alternative to the challenges of autografting (3). Nerve allografts have been demonstrated to preserve the extracellular environment of the injury site (4,5), as well as promoting a favorable environment for local neurotrophic factors to aid in axonal regeneration (6), collectively aiding the biocompatibility of the technique. Though promising, over the previous few decades it has become clear that microsurgical approaches themselves cannot fully reconcile the complex nature of PNI. For this purpose, combinatorial strategies, which employ microsurgical and biological manipulations in tandem (such as neurotrophic factors, extracellular matrix components, over-riding inhibitory cues and cell transplantation), have been increasingly investigated (7,8).

Coupling allografts with growth-enhancing factors has demonstrated improved outcomes compared with unassisted nerve grafts. For example, allografts of the sciatic nerve, when combined with brain-derived neurotrophic factor (BDNF) scaffolding, increased neuronal regeneration in a model of rat

spinal cord injury (9). Similarly, stem cell transplantation is also able to aid PNI recovery, likely due to the multipotent differentiation potential and successful integration into host systems of stem cells, without the need for immunosuppression (10). Bone mesenchymal stem cells (BMSCs) in particular have been demonstrated to aid the regeneration of sciatic nerve injury (11). Previously, we demonstrated that BMSC transplantation combined with chondroitinase ABC (an axonal growth inhibitor-cleaving enzyme) during peripheral nerve allograft enhanced axonal regeneration and functional recovery in a rat model of sciatic nerve injury (12). In general, combinatorial therapies that have been assessed appear to supersede the efficacy of various isolated techniques (7). However, the mechanisms underlying these intervention strategies at the molecular level have yet to be elucidated. Uncovering such strategies is paramount to the optimization of combinatorial therapies and the reduction of adverse outcomes. Herein, we aimed to explore the mechanistic underpinnings of BMSCs and Ch-ABC-assisted acellular allografts on axonal regeneration in peripheral nerve injury. Using a rat model of sciatic nerve gap repair [acellular nerve allograft (ANA)], the cellular, molecular and functional profiles of spinal cord motoneurons, donor nerve, and target tissues were evaluated in order to comprehensively assess the biological outcomes of this combinatorial therapy. The current study describes the direct enhancement of axonal regeneration at the graft site, as well as growth enhancement on spinal cord motoneurons and target organs. These are likely the result of the retro- and anterograde propagation of growth signals sourced from the donor nerve, working in unison to improve observed functional outcomes. The current study reveals a number of the molecular contributors to the therapeutic success of BMSCs and Ch-ABC assisted ANA contributions that may serve as targets for greater investigation and optimization in the future.

Materials and methods

Animals. Healthy Wistar rats (n=48, including 24 male and 24 female) and Sprague-Dawley (SD) rats (n=24, including 12 male and 12 female) weighing 180-220 g were provided by the Experimental Animal Center of China Medical University (Shenyang, China; cert no. SCXK Liao 2008-0005). SD rats were used as nerve donors and Wistar rats were used as graft recipients. The rats were housed in a temperature- and humidity-controlled environment under a 12-h light/dark cycle, with *ad libitum* access to food and water. The animals were housed separately. The present study was approved by the Experimental Animal Administration and Ethics Committee of China Medical University.

Preparation and treatment of ANA. ANA were prepared by a hypotonic chemical detergent method described previously (8). On the day prior to surgery, ANA were incubated with either 100 μl phosphate buffered saline (PBS; pH 7.4) containing 2 U/ml Ch-ABC (Sigma-Aldrich, St. Louis, MO, USA) or with PBS alone (vehicle) for 16 h at 37°C. The grafts were rinsed twice with PBS and stored on ice prior to use.

Preparation of BMSCs. Bone marrow was aspirated with a disposable needle from the femurs of rats sacrificed by CO_2

overdose for preparation of ANA. The cells were collected in heparinized syringes following a previously described protocol (13). Briefly, femurs were removed, cleaned of muscle and connective tissue, and bone marrow was flushed out with PBS. Following centrifugation at 1,000 x g for 5 min at 4°C, the supernatant was discarded and the cells were re-suspended in complete medium containing Dulbecco's modified Eagle's medium (DMEM) supplemented with 10% fetal bovine serum (FBS; Hyclone; GE Healthcare Life Sciences, Logan, UT, USA), 100 U/ml penicillin and 100 U/ml streptomycin at 37°C and 5% CO_2. Following incubation of the dissociated cells for 24 h at 37°C, the non-adherent cells were removed. The adherent cells were continuously cultured at 37°C in 5% CO_2, and then used for the subsequent experiments. In all experiments, cells were used at passages II–IV.

Preparation of ANA seeded with BMSCs. BMSCs were harvested with 0.25% trypsin (Hyclone; GE Healthcare Life Sciences) and suspended in complete medium at a density of $2x10^7$ cells/ml. A total of $2x10^7$ BMSCs in 100 μl complete medium were injected into four evenly spaced points of the nerve section using a micro-injector under an SXP-10 microscope (magnification, x10; Shanghai Medical Equipment Works Co., Ltd., Shanghai, China). The nerve grafts were then incubated in complete medium in a humidified atmosphere containing 5% CO_2 at 37°C for 48 h, after which they were collected for *in vivo* experiments.

Scanning electron microscopy (SEM) analysis. BMSC adhesion to donor ANA was assessed via SEM analysis. Grafts were fixed for 24 h in 4% glutaraldehyde in 0.1 M PBS. The scaffolds were further rinsed in deionized water, and dehydrated with a graded series of ethanol solutions (50, 70, 90, 100%; 10 min each). Finally, the scaffold was treated with hexamethyldisilazane (Sigma-Aldrich) and air-dried in a fume hood overnight. The specimens were mounted on stubs and sputter coated with gold, loaded into a scanning electron microscope (S3400N; JEOL, Ltd., Tokyo, Japan), and viewed under an accelerating voltage of 5 kV.

Additionally, some ANAs were embedded in 1.5% (w/v) agarose (Sigma-Aldrich), fixed in 2% (v/v) glutaraldehyde (Sigma-Aldrich) in 0.1 M phosphate buffer (pH 7.2), post-fixed with 1% (w/v) osmium tetroxide (Sigma-Aldrich), dehydrated in a series of ascending ethanol concentrations, and embedded in epon 812 (Sigma-Aldrich). Ultrathin sections (60 nm) were collected on formvar-coated grids, post-stained with lead citrate and uranyl acetate, and subsequently imaged using electron microscopy (JEOL 1010; JEOL, Ltd.).

Surgical procedures. All Wistar rats were randomly divided into four groups (n=12/group) as follows: Group I, DMEM control group (ANA incubated in DMEM only); Group II, Ch-ABC group (ANA incubated in Ch-ABC only); Group III, BMSCs group (ANA seeded with BMSCs only); Group IV, Ch-ABC + BMSC group (Ch-ABC treated ANA then seeded with BMSCs). In all experiments, the DMEM group served as a negative control. Rats were anesthetized by intraperitoneal injection of 100 g/l chloral hydrate (350 mg/kg weight) and the right sciatic nerve was exposed, the nerve segment was sharply transected, allowed to retract, and then transected

again to bridge a 10-mm defect. The 1-cm acellular nerve grafts were stitched (four pins end-to-end) to bridge the two stumps of the nerve defects with 9-0 nylon sutures under an operation microscope (Fig. 1). The wounds of all rats were rinsed with 40,000 U gentamicin sulfates and muscle and skin were sutured. Following surgery, each rat was assigned an identification number and placed under a warm light, allowed to recover from anesthesia, and then housed separately with access to food and water in a colony room maintained at constant temperature (19-22˚C) and humidity (40-50%) with a 12-h light:dark cycle. No animals were lost to surgical or post-surgical complications.

Immunohistochemistry. Briefly, serial 25 µm-thick frozen sections of the middle nerve graft were cut from each group (n=6) on a cryostat (Leica CM 3000; Leica Microsystems, Inc., Buffalo Grove, IL, USA), mounted on superfrost/plus slides (Menzel-Glaser, Braunschweig, Germany) and incubated with the following primary antibodies for 12 h at 4˚C: Goat anti-nerve growth factor (NGF) polyclonal antibody (1:200 dilution; cat. no. N8773; Sigma-Aldrich), rabbit anti-BDNF polyclonal antibody (1:150 dilution; cat. no. SAB2108004; Sigma-Aldrich), rabbit anti-vascular endothelial growth factor (VEGF) monoclonal antibody (1:150 dilution; cat. no. ab51745; Abcam, Cambridge, MA, USA), rabbit-anti neuronal marker (NeuN) monoclonal antibody (1:200 dilution; cat. no. ab177487; Abcam), mouse anti-choline acetyltransferase (ChAT) monoclonal antibody (1:200 dilution; cat. no. AMAB91129; Sigma-Aldrich) and mouse-anti synaptophysin (SYP) monoclonal antibody (1:200 dilution; cat. no. S5768; Sigma-Aldrich). The immunoreactivity was visualized by incubation with fluorescein isothiocyanate-conjugated goat anti-mouse immunoglobulin (Ig)G (1:200 dilution; cat. no. F0257; Sigma-Aldrich), Texas Red-conjugated goat anti-rabbit IgG (1:200 dilution, cat. no. SAB3700888; Sigma-Aldrich) and CY5-conjugated goat anti-mouse IgG (1:200 dilution; cat. no. SAB4600397; Sigma-Aldrich) for 1 h at room temperature. A MetaMorph/DP10/BX41 analytical imaging system (Olympus Soft Imaging Solutions GmbH, Münster, Germany) was used to scan and generate figures. The integrated optical density (IOD) of positive immunological reactions was also analyzed using Image-Pro Plus 6.0 software (Media Cybernetics, Inc., Rockville, MD, USA). For each section, the positive IOD of five representative visual fields without overlap were observed under a high-power microscope.

The L4 spinal cord was positioned and removed by backward tracking of the repaired nerve. Homolateral tibialis anterior muscles were additionally removed from each group (n=6/group). The tissues were cut as 25 µm-thick frozen serial cross-sections. The sections were incubated in 3% H_2O_2 for 10 min at room temperature then washed carefully with PBS three times (10 min each). The sections were blocked with 5% bovine serum albumin (M B-Chem Corporation, Mumbai, India) for 30 min at 37˚C, then incubated at 4˚C overnight with rabbit anti-NF-200 polyclonal antibody (only for nerve graft; 1:200 dilution; cat. no. N4142; Sigma-Aldrich), goat anti-NGF polyclonal antibody (1:150 dilution), rabbit anti-BDNF polyclonal antibody (1:100 dilution) or rabbit anti-VEGF monoclonal antibody (1:100 dilution). Subsequently, the tissue

Table I. Primer sequences for quantitation of mRNA.

Gene	Sequence	Product size
NGF	Forward: ACCTCTTCGGACACTCTGGA	168 bp
	Reverse: GTCCGTGGCTGTGGTCTTAT	
BDNF	Forward: GGTCACAGTCCTGGAGAAAG	214 bp
	Reverse: GTCTATCCTTATGAACCGCC	
VEGF	Forward: GGACATCTTCCAGGAGTACC	147 bp
	Reverse: CGCATGATCTGCATAGTGAC	

NGF, nerve growth factor; BDNF, brain-derived neurotrophic factor; VEGF, vascular endothelial growth factor.
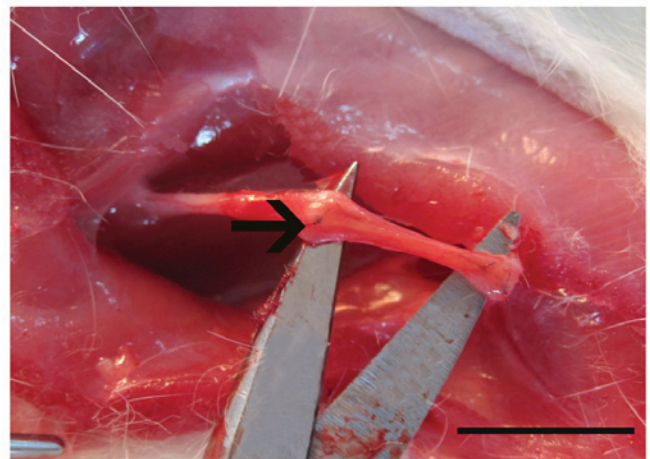

Figure 1. ANA of rat sciatic nerve gap. ANAs (1 cm) were stitched to bridge both stumps of the rat sciatic nerve defects with 9-0 nylon sutures (black arrow) under an operation microscope. Scale bar=10 mm. ANA, acellular nerve allograft.

sections were washed three times in PBS, and then incubated with biotin-labeled goat anti-rabbit IgG (1:200 dilution; cat. no. ZDR-5118; Beijing Zhongshan Jinqiao Biotechnology Co., Ltd., Beijing, China) for 30 min at 37˚C, followed by incubation with streptavidin peroxidase complex (Beijing Zhongshan Jinqiao Biotechnology Co., Ltd.) for 30 min at 37˚C. Following washing with PBS and staining with 3,3-diaminobenzidine (Sigma-Aldrich) for 10 min, the tissue sections were observed under a light microscope (DM3000; Leica Microsystems GmbH, Wetzlar, Germany). The positively stained motoneurons in the spinal cord anterior horn were counted, and the integrated optical density of positively stained nerves and muscles was analyzed using an analytical imaging system (Olympus Soft Imaging Solutions GmbH).

Reverse transcription-quantitative polymerase chain reaction (RT-qPCR). Total RNA was extracted from the nerve graft, spinal cord and muscles using TRIzol reagent (Invitrogen; Thermo Fisher Scientific, Inc., Waltham, MA, USA) according to the manufacturer's protocol (n=6/group). Purified RNA was diluted to 500 ng/µl and 3 µl RNA was used to synthesize cDNA with a Prime Script RT reagent kit

(Takara Biotechnology Co., Ltd., Dalian, China). Primers were designed and synthesized by Takara Biotechnology Co., Ltd., and their sequences are displayed in Table I. RT-qPCR was performed using a SYBR Premix Ex *Taq* kit (Takara Biotechnology Co., Ltd.) according to the manufacturer's protocol for qPCR systems (ABI Prism 7000; Applied Biosystems; Thermo Fisher Scientific, Inc.). The amplification conditions were as follows: 30 sec at 95°C (one cycle), 5 sec at 95°C and 30 sec at 60°C (40 cycles) followed by 72°C for 5 min (one cycle). RT-qPCR was performed three times in triplicate to evaluate the reproducibility of the data. The cycle number at which the amplification curve crossed the threshold line was noted as the critical quantification (Cq) and gene expression was calculated by the comparative Cq ($2^{-\Delta\Delta Cq}$) method, using β-actin as the housekeeping gene for normalization.

Motoneurons, dendritic number and morphology. Eight weeks after injury, the rats were re-anesthetized and the left vastus lateralis muscle of the quadriceps was exposed and injected with horseradish peroxidase (HRP) conjugated to the cholera toxin B subunit (BHRP; 2 µl; 0.2%; List Biological Laboratories, Inc., Campbell, CA, USA). BHRP labeling permits population level quantitative analysis of motoneuron soma and dendritic morphology. Following BHRP injection [(48 h after, in order to ensure optimal labeling of motoneurons (14,15)], the rats were weighed and received a lethal dose of Nembutal (45 mg/kg, i.p.; Sigma-Aldrich). The rats were subsequently perfused intracardially with saline followed by cold fixative solution (1% paraformaldehyde/1.25% glutaraldehyde), and then cut on a cryostat (40-µm-thick transverse sections for spinal cords).

Motoneurons and dendritic lengths in a single representative set of alternate L4 spinal cord sections were measured under darkfield illumination initiated with the first section in which BHRP-labeled motoneurons and fibers were present. Labeling throughout the entire rostrocaudal extent of the quadriceps motoneuron dendritic field was assessed in each section using a computerized morphometry system (Neurolucida; MBF Bioscience, Inc., Williston, VT, USA) at a final magnification x250. No attempt was made to distinguish BHRP-labeled fibers as either dendrites or axons. Average dendritic length per labeled motoneuron was estimated by totaling the measured dendritic lengths of the serial sections, multiplying by three to correct for sampling error, and then dividing by the total number of labeled motoneurons that was detected in that series (16). The length of labeled dendrites of motoneurons was assessed in sections 320 µm apart through the length of the lumbar spinal cord. A total of six rats were analyzed per group.

Electrophysiological analysis. Electrophysiological analysis was performed on the rats prior to sacrifice by CO_2 overdose, using a Haishen NDI-200P1 electroneurogram device (Shanghai, China). The stimulus intensity was 1-20 mA to ensure a maximum waveform and to prevent independent muscle contractions. The stimulus duration was 0.1-0.2 msec, and the stimulation frequency was 1 Hz. Subsequently, with each animal under general anesthesia (pentobarbital; 60 mg/ml i.p. injection; Sigma-Aldrich) the right sciatic nerve was exposed. A crook-shaped silver needle electrode was placed on the proximal and distal ends of the grafts, which were then stimulated at the distal end and recorded at the proximal end. The distance between the two electrodes was measured with a sliding caliper with 0.2 mm precision. Nerve conduction velocity, latency period and wave amplitude were then recorded in eight rats from each group.

Tibialis anterior muscle weights. The tibialis anterior muscles were dissected from both sides and detached from the bone at their origin and terminal point following electrophysiological analysis, and weighed immediately with an electron scale to 0.0001 precision. The weight on the operated side was expressed as a percentage of the muscle weight on the unoperated side.

Statistical analysis. All quantitative data were expressed as means ± standard deviation and analyzed with SPSS statistical software (version 13.0; SPSS, Inc., Chicago, IL, USA). One-way analysis of variance followed by Dunnett's test was used for the comparison among experimental groups. Non-parametric data were compared using the Mann-Whitney U test among experimental groups. P<0.05 was considered to indicate a statistically significant difference.

Results

BMSC cultures and secreted growth factor. BMSCs appeared suspended in culture medium on day 1 and exhibited a small, spindle-like or fibroblast-like morphology on day 3. Cells reached 90% confluence on day 7. By the 3rd passage, BMSCs began to exhibit a whirlpool-like arrangement (Fig. 2A-D). After 5 days of co-culture of BMSCs with DMEM or Ch-ABC-treated ANA, SEM observation revealed that BMSCs attach tightly to ANA irrespective of pretreatment with ANA (Fig. 2E-F). Subsequent to 5 days of co-culture, the growth factors NGF, BDNF and VEGF were investigated in pre-grafted ANA. Growth factors were detected at higher levels in the BMSC and Ch-ABC + BMSC groups compared with the DMEM group and Ch-ABC groups. No significant difference was observed between the Ch-ABC group and the DMEM group, nor did the addition of Ch-ABC to BMSC seeded ANA appear to enhance the growth factor response (Fig. 2G), indicating that, at least pre-operatively, BMSCs are primarily responsible for the stimulation of growth on the donor nerve.

Combination treatment promotes axon regeneration. Immunohistochemical staining was performed for a nerve fiber marker (NF-200) in ANA in 4 and 8 week post-operative nerve recipients. It was revealed that the number of nerve fibers was significantly increased in all treatment groups compared with the DMEM negative control at 4 and 8 weeks (P<0.05; Fig. 3). Notably, the number of nerve fibers in the Ch-ABC + BMSCs group was greater compared with the Ch-ABC and BMSC groups (P<0.05; Fig. 3). The aforementioned results indicate that combined BMSCs and Ch-ABC treatment promotes axonal regeneration at a greater capacity than any single treatment of the ANA 4-8 weeks after grafting.

Combination therapy promotes NGF, BDNF and VEGF expression in the regenerated tissues. Immunofluorescence
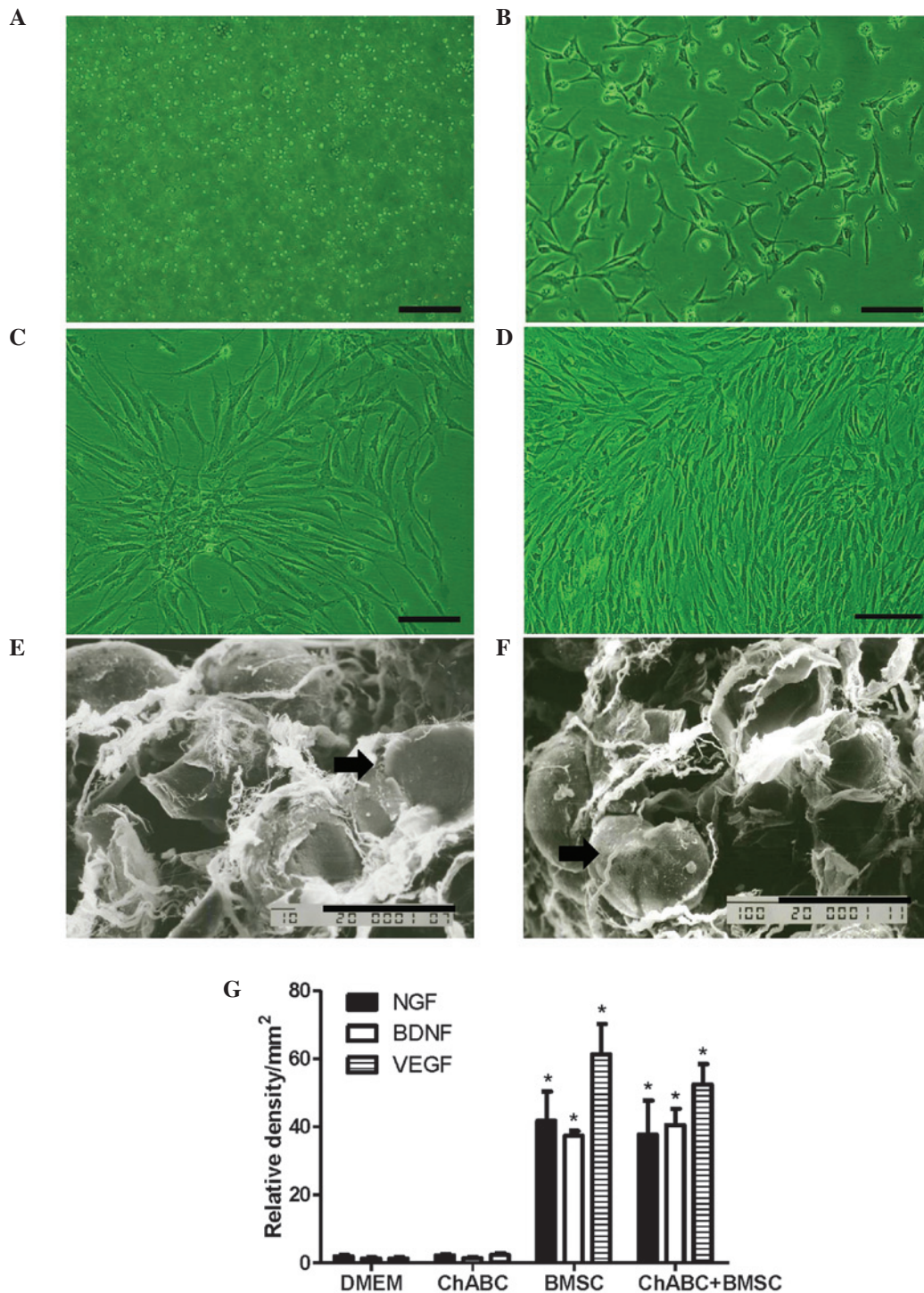
Figure 2. BMSC culture and adherence to ANA. BMSCs were cultured at (A) day 1, (B) day 3, (C) day 7 and (D) at passage III (Scale bar=20 μm). SEM evaluation of BMSCs (black arrow) revealed (E) adhesion to the ANA and (F) Ch-ABC incubated ANA *in vitro* (Scale bar=10 μm). Analysis of NGF, BDNF and VEGF immunoreactivity in ANA sections was determined by integrated optical density. (G) NGF, BDNF and VEGF relative densities. n=6 per treatment condition. All data are expressed as means ± standard deviation. *P<0.05, vs. the DMEM group. ANA, acellular nerve allografts; SEM, scanning electron microscope; BMSC, bone marrow stromal cell; Ch-ABC, chondroitinase ABC; DMEM, Dulbecco's modified Eagle's medium; NGF, nerve growth factor; BDNF, brain-derived neurotrophic factor; VEGF, vascular endothelial growth factor.

analysis revealed that in the centre of the ANA, NGF, BDNF and VEGF protein expression levels were increased in the BMSC and ChABC + BMSC groups compared with the DMEM and Ch-ABC groups (P<0.05; Fig. 4). Across all growth factors, the addition of Ch-ABC pre-treatment further increased the expression levels of the growth factors, compared with the BMSC group (P<0.05). Motoneurons of the L4 spinal cord anterior horn (Fig. 5) and target muscle tissue (Fig. 6) were similarly examined and resulted in similar growth factor expression patterns as the ANA (P<0.05). The immunohisto-chemical data demonstrates the local and distal generation of growth factor responses primarily to BMSC seeding of the graft, with a level of additional enhancement due to Ch-ABC pre-treatment of the ANA.
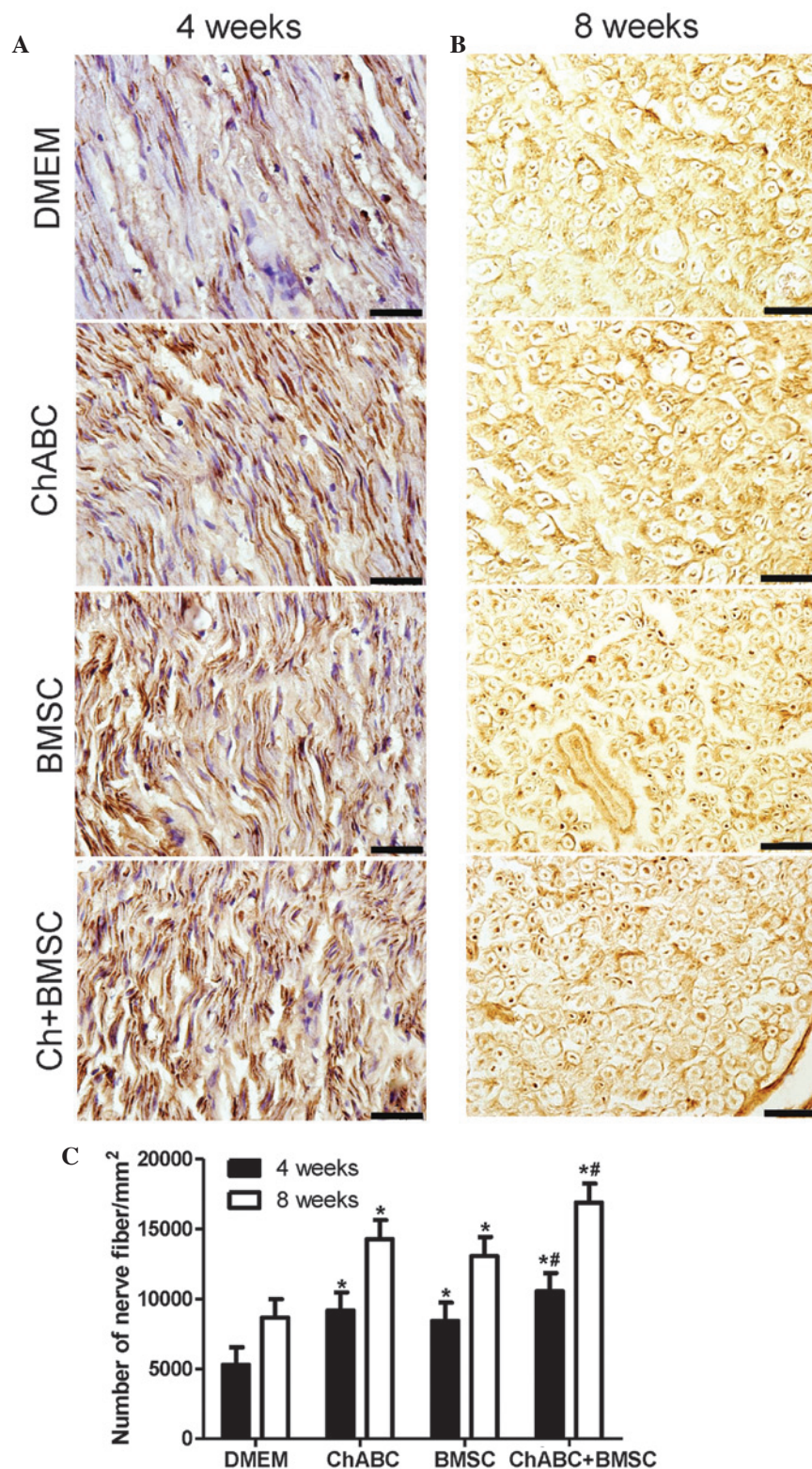
Figure 3. Longitudinal assessment of post-graft axonal regeneration. Immunohistochemical staining of neurofilament protein was performed in sections obtained from mid acellular nerve allograft from each group, collected at (A) 4 weeks (longitudinal section) and (B) 8 weeks (transverse section) (Scale bar=20 μm). (C) The number of nerve fibers. All data are expressed as the mean ± standard deviation; *P<0.05, vs. the DMEM group; #P<0.05, vs. the BMSC group; n=6 per group. BMSC, bone marrow stromal cell; Ch-ABC, chondroitinase ABC; DMEM, Dulbecco's modified Eagle's medium.

RT-qPCR analysis indicated that the comparative patterns of NGF, BDNF and VEGF mRNA expression levels in the ANA, L2-4 spinal cord and distal muscles were generally consistent with their comparative protein expression patterns. NGF, BDNF and VEGF mRNA expression levels in the BMSC group and Ch-ABC + BMSC group were higher compared with the DMEM and Ch-ABC groups (P<0.05) when ANA mRNA expression levels were analyzed (Fig. 7A). Spinal cord and muscle mRNA analysis indicated similar patterns of expression for BDNF, VEGF and NGF (Fig. 7B and C).
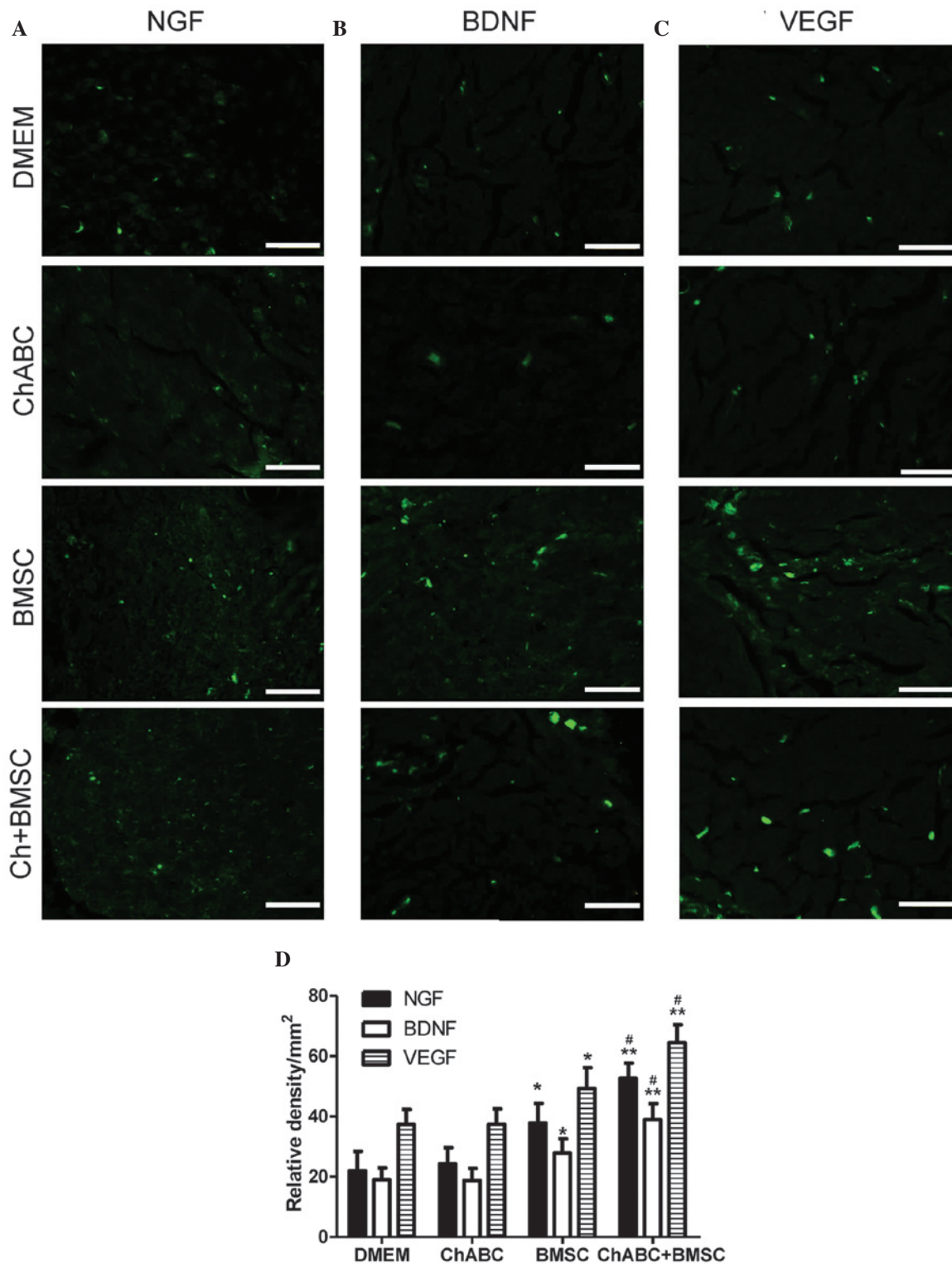
Figure 4. Immunohistochemical analysis of growth factor abundance in ANA 8 weeks after grafting. Immunohistochemical staining of (A) NGF, (B) BDNF and (C) VEGF in mid ANA sections across all treatment groups. Optical detection of immunoreactivity was achieved by green fluorescent reporter (Scale bar=20 μm). (D) Relative densities of immunoreactivity. All data are expressed as means ± standard deviation. *P<0.05, **P<0.01 vs. the DMEM group; #P<0.05 vs. the BMSC group. n=6 per group. BMSC, bone marrow stromal cell; Ch-ABC, chondroitinase ABC; DMEM, Dulbecco's modified Eagle's medium; ANA, acellular nerve allograft; NGF, nerve growth factor; BDNF, brain-derived neurotrophic factor; VEGF, vascular endothelial growth factor.

Detected across all tissues examined was the enhancement of the mRNA expression levels of NGF, BDNF and VEGF for the combined group BMSC + Ch-ABC compared with the BMSC group (P<0.05). Conclusively, the aforementioned results indicate that combination therapy is able to increase growth factor

protein and mRNA expression levels in the ANA, and across the distal spinal cord and target tissue sites.

Combination therapy protects motoneurons. Immunohistochemical staining was performed to detect the
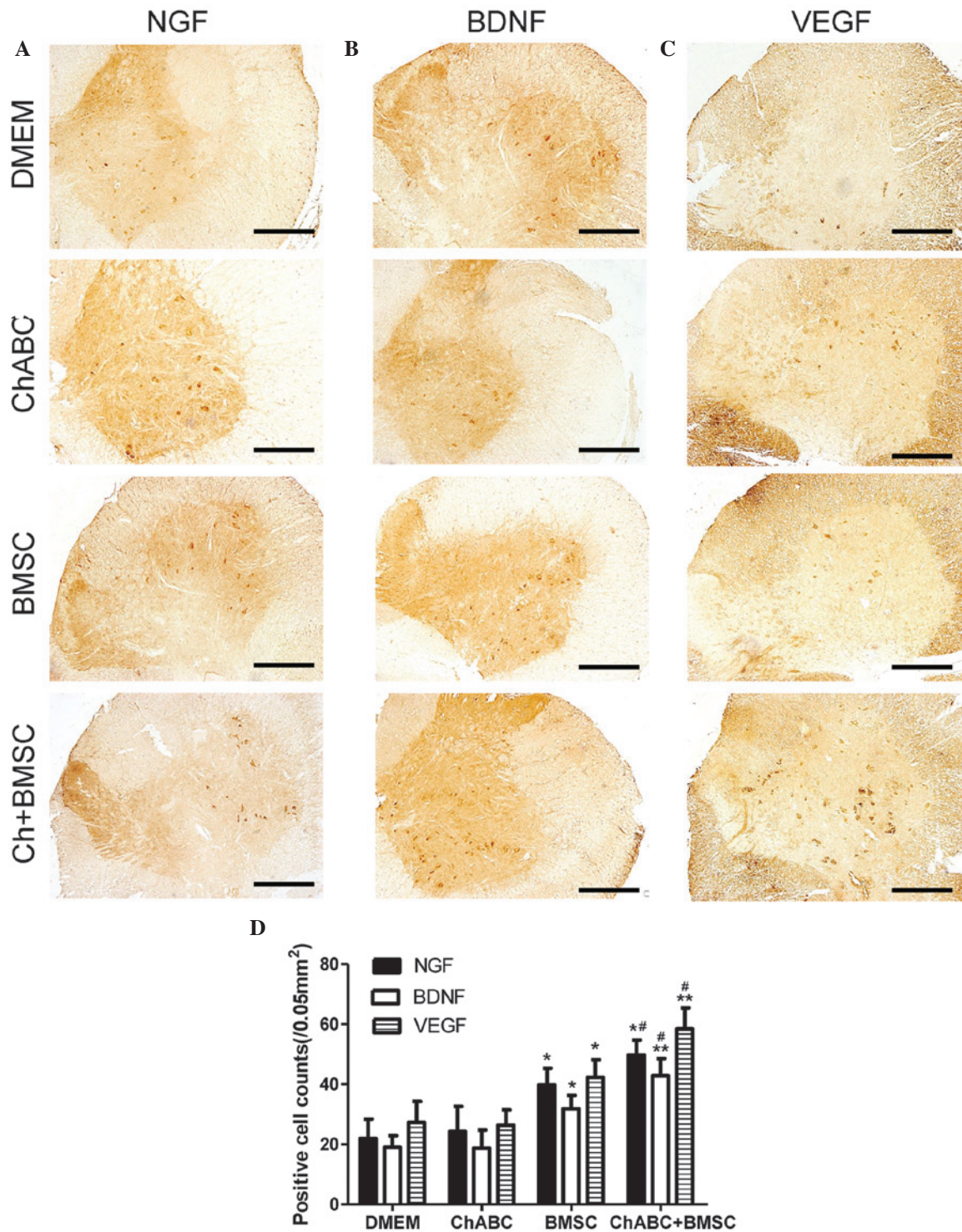
Figure 5. Immunohistochemical staining of (A) NGF, (B) BDNF and (C) VEGF in the L4 spinal cord. 8 weeks after grafting (Scale bar=100 μm). (D) The numbers of positively stained neurons counted across sections of the spinal cord. All data are expressed as means ± standard deviation. *P<0.05, **P<0.05 vs. the DMEM group, $^{#}$P<0.05, vs. the BMSC group. n=6 per group. BMSC, bone marrow stromal cell; Ch-ABC, chondroitinase ABC; DMEM, Dulbecco's modified Eagle's medium; NGF, nerve growth factor; BDNF, brain-derived neurotrophic factor; VEGF, vascular endothelial growth factor.

NeuN, motoneuron marker (ChAT), SYP, and HRP retrograde labeled motoneurons and dendrites in the L5 spinal cord. It was revealed that the number of NeuN and ChAT-positive neurons and synaptophysin protein expression was significantly increased in the Ch-ABC, BMSC and Ch-ABC + BMSC groups compared with the DMEM group at 8 weeks (P<0.05). Notably, the number of NeuN and ChAT-positive neurons, and synaptophysin-positive relative density in the Ch-ABC + BMSC group were much greater compared with the Ch-ABC group or the BMSC group (P<0.05; Fig. 8).

Molecular indicators of neuronal growth and protection can be used to demonstrate the functional recovery of an artificial nerve alongside morphological indicators of axonal growth. Specifically, the motoneuron area, dendritic segment length
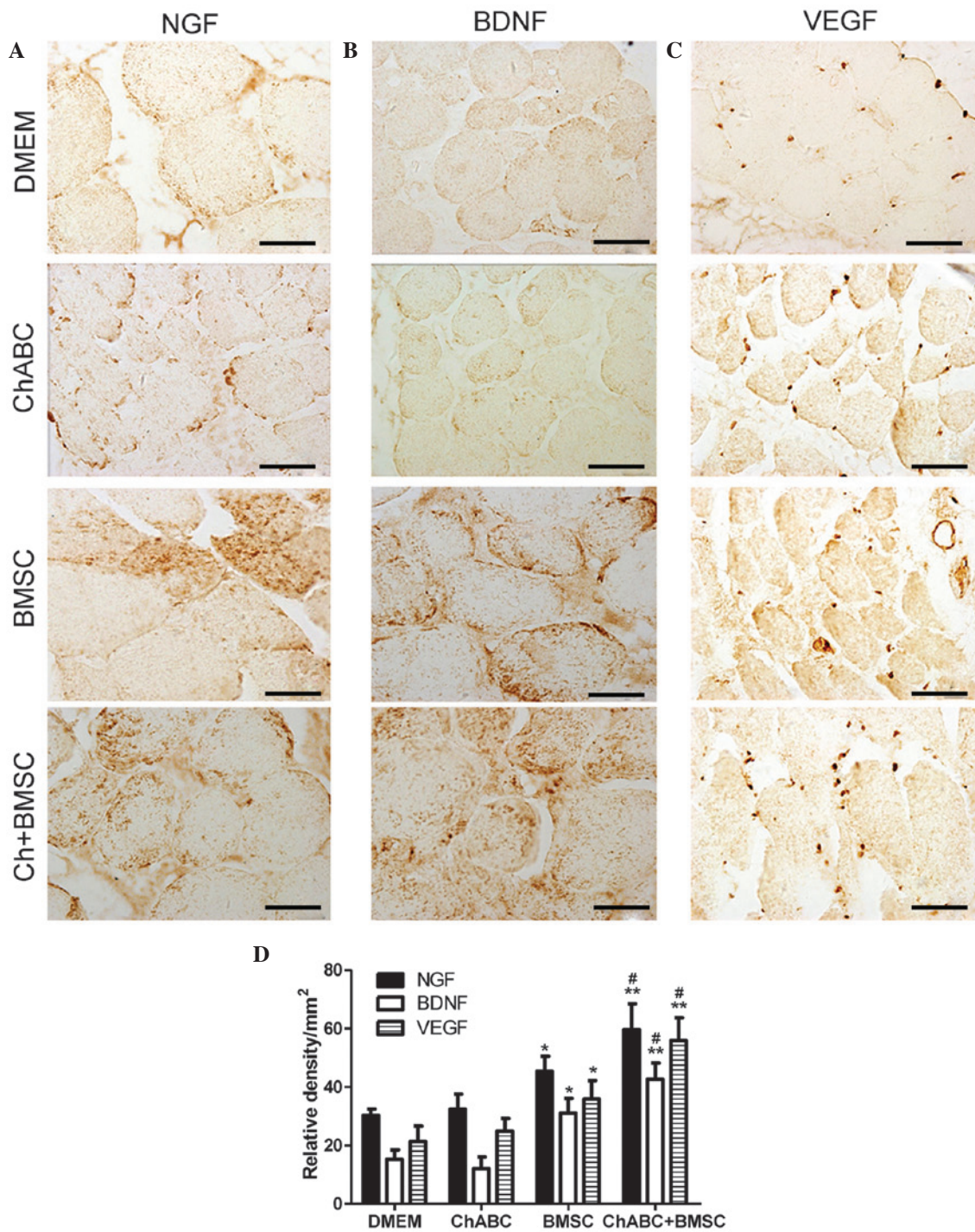
Figure 6. Immunohistochemical analysis of NGF, BDNF and VEGF in the anterior tibial muscles. 8 weeks after grafting, target muscle organ sections from each group were assessed for (A) NGF, (B) BDNF and (C) VEGF immunoreactivity (Scale bar=20 μm). (D) Relative density of positive signals. All data are expressed as means ± standard deviation. *P<0.05, **P<0.01 vs. the DMEM group; #P<0.05 vs. the BMSC group. n=6 per group. BMSC, bone marrow stromal cell; Ch-ABC, chondroitinase ABC; DMEM, Dulbecco's modified Eagle's medium; NGF, nerve growth factor; BDNF, brain-derived neurotrophic factor; VEGF, vascular endothelial growth factor.

and total dendritic length exhibited greater values in the BMSC, Ch-ABC and BMSC + Ch-ABC treated ANA compared with DMEM negative control. Thus, this further confirms previous results indicating that the BMSC + Ch-ABC group displayed significantly higher values compared with all other groups (P<0.05; Fig. 8). The results suggest that combined BMSCs and Ch-ABC treatment optimally protects motoneurons and enhances dendritic profiles following injury.

Combined treatment promotes the recovery of sciatic nerve function. At 8 weeks post-surgery, the conduction velocity (Fig. 9A), latency period (Fig. 9B) and wave amplitude (Fig. 9C) of the nerve graft were assessed by electrophysiology. The conduction velocity (Fig. 9A) and wave amplitude (Fig. 9C) were higher in all treatment groups compared with DMEM negative controls. Ch-ABC + BMSC combined treatment increased the values above BMSC or Ch-ABC alone (P<0.05).
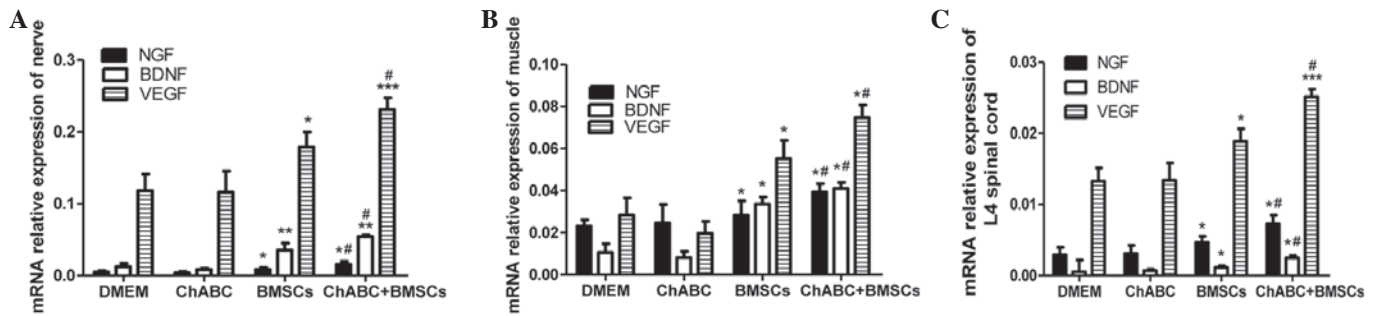
Figure 7. mRNA expression of NGF, BDNF and VEGF. 8 weeks after grafting, (A) ANA, (B) spinal cord and (C) anterior tibial muscles were extracted from all treatment groups for quantitation of NGF, BDNF and VEGF relative expression . mRNA expression was determined by reverse transcription-quantitative polymerase chain reaction. All data are expressed as means ± standard deviation. *P<0.05, **P<0.01, ***P<0.001, vs. the DMEM group; #P<0.05, vs. the BMSC group; (n=6). BMSC, bone marrow stromal cell; Ch-ABC, chondroitinase ABC; DMEM, Dulbecco's modified Eagle's medium; NGF, nerve growth factor; BDNF, brain-derived neurotrophic factor; VEGF, vascular endothelial growth factor.

Conversely, the latency period (Fig. 9B) was decreased significantly in all treatment groups compared with the DMEM control group (P<0.05). Furthermore, the latency period was decreased to a greater extent in the Ch-ABC + BMSC group compared with the Ch-ABC and BMSC group (P<0.05). A final investigation of the recovery of tibialis anterior muscle weights (Fig. 9D) corroborated the effectiveness of either Ch-ABC or BMSC treatment while reinforcing that the combinatorial treatment supersedes the muscle recovery of either (P<0.05). These results support the hypothesis that while BMSC and Ch-ABC alone contributed to functional recovery of the nerve graft in vivo, the combination of the two therapies enhances the recovery rate significantly.

Discussion

There is an increasing necessity in the field of PNI for therapies with improved long-term outcomes. Biologically, this equates to the requirement of novel and more efficacious methods of axonal regeneration. Recently, it has been demonstrated that the complex aberrations of PNI are better treated with a combination of peripheral nerve grafting and growth-promoting factors (such as stem cell transplantation and growth factor enhancement) (17). Despite improvements in functional and anatomical parameters of recovery, little is understood about the molecular drivers of combinatorial therapy such as Ch-ABC and BMSC-assisted ANA. Identifying the molecular growth cues of peripheral nerve regeneration, and how these may be enhanced by therapies such as stem cell transplantation and axonal growth factors may assist with the stratification of the adverse outcomes of nerve grafting, and guide future therapeutic intervention. Molecular, anatomical and functional parameters of peripheral nerve injury recovery were evaluated in the present study, subsequent to the establishment of a model of ANA pretreated with Ch-ABC and seeded with BMSCs.

BMSCs adhere tightly to donor ANA and stimulate the expression of NGF and BDNF growth factors in vitro. This signifies that even prior to surgery, the presence of multipotent stem cells is already enhancing the ability of the donor nerve to secrete growth-permissive factors (12). This 'priming' may ultimately contribute to the biocompatibility of the donor graft to the recipient. BMSC seeding of the ANA serves to continually improve growth factor secretion in vivo with Ch-ABC

significantly enhancing NGF, VEGF and BDNF secretion post-transplantation. The latter is likely due to the function of Ch-ABC as a remover of proteoglycan obstructions impeding axonal growth, and is a probable explanation for the absence of a Ch-ABC growth enhancement in vitro.

To the best of our knowledge, the present study reports for the first time that BMSC and BMSC + Ch-ABC treatments enhance the growth factor responses at distal sites of the ANA, at the spinal cord and target muscle, in a rat model of sciatic nerve gap. The patterns observed at distal sites reflect growth factor expression at the graft site, indicating that the propagation of growth cues occurs bidirectionally. Notably, retrograde axonal transport of growth factors, such as BDNF and NT-3, has previously been observed in spinal cord motoneurons with a distinct selectivity (18). Anterograde axonal transport of the neurotrophic factor, leukemia inhibitory factor, to denervated muscle was previously observed in a model of sciatic nerve transection (19), thus suggesting that neurotrophins such as BDNF, NGF and VEGF may also accumulate in target organs such as muscle. In 2001, von Bartheld et al (20) proposed several intricate, multi-step transfers of neurotrophic factors across neural circuits, a number of which may fit within the observed axonal anterograde transport and even reach dendritic fields. Ultimately, this bidirectional propagation of growth signals is likely an important contributor to the cellular and functional recovery observed after injury in previous BMSC + Ch-ABC treatment models (12).

Combining the aforementioned data, the growth signal enhancement of the ANA, spinal cord and target muscle converge to guide axonal regeneration, neuronal protection and functional recovery.

The synergistic effect of local and distal growth signaling manifest therapeutic benefits, such as the observed nerve fiber growth that occurs on the ANA, up to 8 weeks after grafting (Fig. 3). Additionally, spinal cord motoneurons benefit through increased expression of mature neuronal markers and motoneuron specifiers (Fig. 5). The indicated increase in motoneuron survival has previously been observed in intramuscular stem cell transplantation models, suggesting that spinal cord motoneuron survival is assisted by growth factor-secreting stem cells acting locally (21), or as far as target muscular regions (22). It is plausible then, that BMSC and BMSC + Ch-ABC, promoting growth factor secretion at local
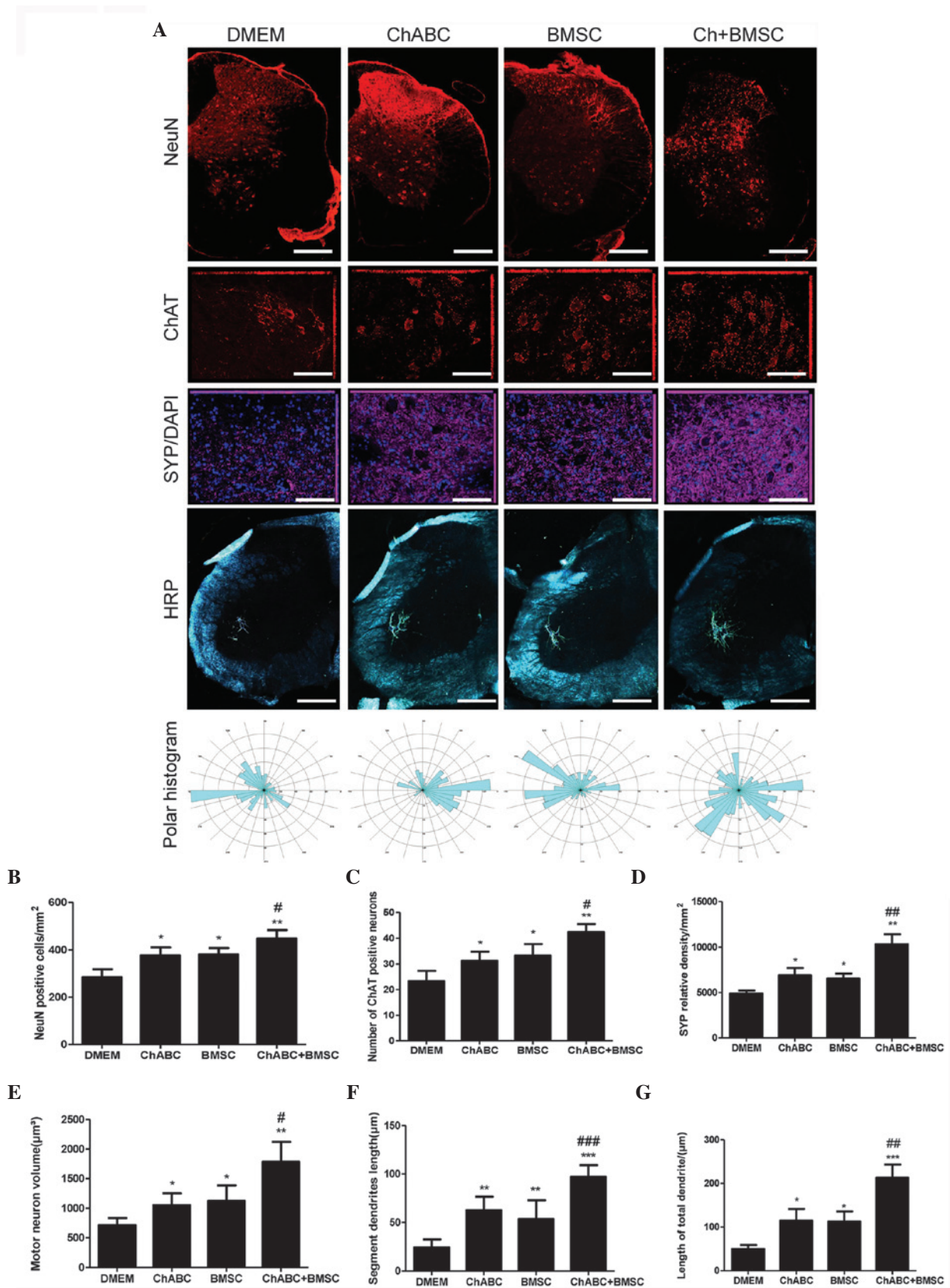
Figure 8. Motoneuron survival and dentritogenesis in the L4 spinal cord 8 weeks after graft: (A) Immunohistochemical staining of NeuN (Scale bar=100 μm), ChAT (Scale bar=20 μm) and synaptophysin (Scale bar=20 μm). DAPI nuclear counterstain (blue) was performed on L4 spinal cord sections across treatment groups using fluorescent reporters. Below, horseradish peroxidase retrograde tracing of motoneuron dendrites in the L4 spinal cord (Scale bar=100 μm) were generated by injection with B-horseradish peroxidase 4 weeks after injury (analyzed 48 h after injection). Polar histograms of dendritic fields were generated by computer morphometry system across the various groups. Numbers of (B) NeuN and (C) ChAT-positively stained neurons are counted and in (D) synaptophysin relative density of the spinal cord is displayed. (E) Area of motoneurons is displayed, and (F) the segment lengths of the motoneuron dendrites as well as total dendritic lengths (G) are also presented. Data are expressed as means ± standard deviation; $^{*}P<0.05$, $^{**}P<0.01$, $^{***}P<0.001$, vs. the DMEM group. $^{#}P<0.05$, $^{##}P<0.01$, $^{###}P<0.001$, vs. the BMSC group. n=6 per group). BMSC, bone marrow stromal cell; Ch-ABC, chondroitinase ABC; DMEM, Dulbecco's modified Eagle's medium; ChAT, choline acetyltransferase; NeuN, neuronal marker.
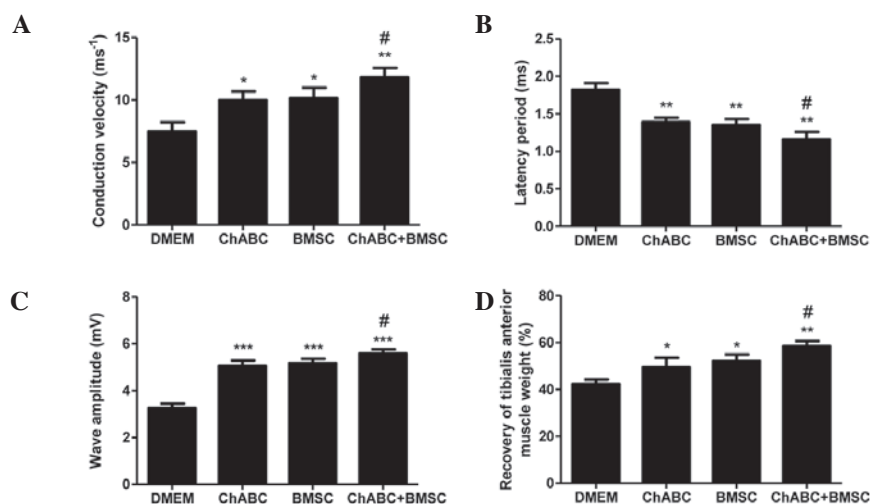
Figure 9. Electrophysiological index and tibialis anterior muscle recovery. (A) Conduction velocity, (B) latency period, (C) wave amplitude of the nerve graft were assessed by electrophysiology prior to sacrifice (8 weeks after graft). (D) Recovery assessment of tibialis anterior muscle was also indicated by the weight ratio of muscle from operated side to the muscle weight of the un-operated (contralateral) side. All data expressed as mean ± standard deviation. *P<0.05, **P<0.01, ***P<0.001, vs. the DMEM group; $^#$P<0.05, vs. the BMSC group; (n=8 per group). BMSC, bone marrow stromal cell; Ch-ABC, chondroitinase ABC; DMEM, Dulbecco's modified Eagle's medium; NGF, nerve growth factor; BDNF, brain-derived neurotrophic factor; VEGF, vascular endothelial growth factor.

and/or distal ends of the allograft, are similarly supporting motoneuron survival.

Furthermore, the use of combinatorial ANA therapies administered in the current study indicated that synaptic profiles of motoneuron dendrites were markedly improved (Fig. 8). Similarly, the synaptic protein synaptophysin is enhanced by BMSC + Ch-ABC treatment. Retrograde transport of neurotrophic factors such as BDNF has previously demonstrated the capacity to reach motoneuronal synaptic sites through a process called transsynaptic transcytosis (23), activating a cascade of synaptic plasticity signals. Another previous study reported that mesenchymal stem cell secretion of BDNF and GDNF at spinal motoneuron sites aided synaptophysin-positive nerve terminal preservation (24) and motoneuron synaptogenesis (21). Ultimately, survival and synaptogenesis of the motoneuron are critical to functional reinnervation of target tissue, and molecular mechanisms such as those used in the model in the current study likely enhance functional recovery.

Functional parameters of axonal regeneration have been previously demonstrated in our BMSC + Ch-ABC model of ANA (8); however, the molecular underpinnings had yet to be elucidated. In the current study, it was revealed that electrophysiological measures of recovered nerve function are improved, likely as an effect of the local and retro/anterograde transport of BMSC-assisted growth factors (Fig. 9). In addition, removal of proteoglycan obstructions by Ch-ABC contributes to an enhanced functional recovery. The mechanism by which growth signals trigger axonal regeneration remains subject to debate. Live, long-term imaging of axonal lesions has demonstrated that growth factors such as BDNF are able to promote cytoskeletal elements responsible for cell growth (25). Specifically, the number and rate of actin 'waves' that form the microfilaments responsible for axonal morphogenesis and pathfinding, are enhanced by the introduction of BDNF (26).

Finally, the present study reported that the restoration of target muscle mass is innervated by axotomized nerves.

Muscular growth and reinnervation are critical components of functional recovery from PNI. Graft site stimulation of growth cues were anterogradely propagated to muscle targets. Gene manipulation-derived delivery of the growth factor VEGF has previously been demonstrated to aid in peripheral nerve regeneration through the enhancement of nerve reinnervation and axonal diameter growth (27). Similarly, VEGF intervention in a PNI model demonstrated that denervated muscle atrophy was significantly slowed, although VEGF overexpression led to worse nerve regeneration compared with negative controls (28).

Notably, although Ch-ABC and BMSC contributed to the functional recovery of the nerve, the combination of the two outweighed the therapeutic benefit of each treatment individually in almost all parameters of morphological and functional recovery assessed by the current study. This effect is enduring and abounds not only in the graft site but extends to both distal regions where the target muscle and motoneurons also demonstrate therapeutic phenomena. In the current study, the first reported comprehensive molecular examination of the BMSC + Ch-ABC ANA in an *in vivo* model of sciatic nerve gap was attempted. It was determined that the combination therapy enhances the growth response of the nerve, however, also appears to stimulate the growth response of the target organ and motoneurons. The aforementioned wide-reaching stimulation of growth factors ultimately contributes to functional repair of not only the nerve, but also the protection of the motoneuron and the growth of the target muscle.

Although the current study improved our understanding of the molecular cues guiding nerve regeneration in Ch-ABC + BMSC ANA repair, the method by which growth signals are propagated to the distal ends of the graft remains unclear. We propose retro- and anterograde transport pathways as a plausible means of growth signal propagation, though a thorough examination of these mechanisms remains to be performed. Furthermore, the convergence of distal and local growth signals render it difficult to reveal the exact method by

which each signaling source is mechanistically associated with individual parameters of post-graft recovery. It will be important in the future to analyze these independently to better gauge how each signaling source specifically contributes to cellular and functional aspects of recovery. Investigation of growth factor-activated downstream signaling is also important to further understand the exact signaling pathways that mediate anatomical and functional restoration such as neurite growth. Pharmacological manipulation and time-course designs are potential approaches to further investigate the results reported in the current study. Despite limitations, it is clear that an understanding of how BMSCs and Ch-ABC mediate growth signaling affects and enhance donor nerve growth cues is a step toward optimizing the combinatorial therapy that has to date demonstrated marked efficacy. This endeavor is worthwhile as a full functional recovery of peripheral nerve injury remains to be achieved.

Acknowledgements

References

1. Johnson EO, Zoubos AB and Soucacos PN: Regeneration and repair of peripheral nerves. Injury 36 (Suppl 4): S24-S29, 2005.
2. Millesi H: Bridging defects: Autologous nerve grafts. In: How to improve the results of peripheral nerve surgery. Vol. 100. Millesi H and Schmidhammer R (eds). Springer, Vienna, pp37-38, 2007.
3. Tang P and Chauhan A: Decellular Nerve Allografts. J Am Acad Orthop Surg 23: 641-647, 2015.
4. Zhang C, Yao C, He XJ and Li HP: Repair of subacute spinal cord crush injury by bone marrow stromal cell transplantation and chondroitinase ABC microinjection in adult rats. Nan Fang Yi Ke Da Xue Xue Bao 30: 2030-2035, 2010 (In Chinese).
5. Zhang LX, Tong XJ, Sun XH, Tong L, Gao J, Jia H and Li ZH: Experimental study of low dose ultrashortwave promoting nerve regeneration after acellular nerve allografts repairing the sciatic nerve gap of rats. Cell Mol Neurobiol 28: 501-509, 2008.
6. Côté MP, Amin AA, Tom VJ and Houle JD: Peripheral nerve grafts support regeneration after spinal cord injury. Neurotherapeutics 8: 294-303, 2011.
7. Zhang Y, Zhang H, Zhang G, Ka K and Huang W: Combining acellular nerve allografts with brain-derived neurotrophic factor transfected bone marrow mesenchymal stem cells restores sciatic nerve injury better than either intervention alone. Neural Regen Res 9: 1814-1819, 2014.
8. Jia H, Wang Y, Tong XJ, Liu GB, Li Q, Zhang LX and Sun XH: Sciatic nerve repair by acellular nerve xenografts implanted with BMSCs in rats xenograft combined with BMSCs. Synapse 66: 256-269, 2012.
9. Li C, Zhang X, Cao R, Yu B, Liang H, Zhou M, Li D, Wang Y and Liu E: Allografts of the acellular sciatic nerve and brain-derived neurotrophic factor repair spinal cord injury in adult rats. PLoS One 7: e42813, 2012.
10. Wang Y, Zhao Z, Ren Z, Zhao B, Zhang L, Chen J, Xu W, Lu S, Zhao Q and Peng J: Recellularized nerve allografts with differentiated mesenchymal stem cells promote peripheral nerve regeneration. Neurosci Lett 514: 96-101, 2012.
11. Chen CJ, Ou YC, Liao SL, Chen WY, Chen SY, Wu CW, Wang CC, Wang WY, Huang YS and Hsu SH: Transplantation of bone marrow stromal cells for peripheral nerve repair. Exp Neuro 204: 443-453, 2007.
12. Wang Y, Jia H, Li WY, Tong XJ, Liu GB and Kang SW: Synergistic effects of bone mesenchymal stem cells and chondroitinase ABC on nerve regeneration after acellular nerve allograft in rats. Cell Mol Neurobiol 32: 361-371, 2012.
13. Sanchez-Ramos J, Song S, Cardozo-Pelaez F, Hazzi C, Stedeford T, Willing A, Freeman TB, Saporta S, Janssen W, Patel N, et al: Adult bone marrow stromal cells differentiate into neural cells in vitro. Exp Neurol 164: 247-256, 2000.
14. Goldstein LA, Kurz EM and Sengelaub DR: Androgen regulation of dendritic growth and retraction in the development of a sexually dimorphic spinal nucleus. J Neurosci 10: 935-946, 1990.
15. Kurz EM, Bowers CA and Sengelaub DR: Morphology of rat spinal motoneurons with normal and hormonally altered specificity. J Comp Neurol 292: 638-650, 1990.
16. Byers JS, Huguenard AL, Kuruppu D, Liu NK, Xu XM and Sengelaub DR: Neuroprotective effects of testosterone on motoneuron and muscle morphology following spinal cord injury. J Comp Neurol 520: 2683-2696, 2012.
17. Zhang YR, Ka K, Zhang GC, Zhang H, Shang Y, Zhao GQ and Huang WH: Repair of peripheral nerve defects with chemically extracted acellular nerve allografts loaded with neurotrophic factors-transfected bone marrow mesenchymal stem cells. Neural Regen Res 10: 1498-1506, 2015.
18. DiStefano PS, Friedman B, Radziejewski C, Alexander C, Boland P, Schick CM, Lindsay RM and Wiegand SJ: The neurotrophins BDNF, NT-3, and NGF display distinct patterns of retrograde axonal transport in peripheral and central neurons. Neuron 8: 983-993, 1992.
19. Bennett TM, Dowsing BJ, Austin L, Messina A, Nicola NA and Morrison WA: Anterograde transport of leukemia inhibitory factor within transected sciatic nerves. Muscle Nerve 22: 78-87, 1999.
20. von Bartheld CS, Wang X and Butowt R: Anterograde axonal transport, transcytosis, and recycling of neurotrophic factors: The concept of trophic currencies in neural networks. Mol Neurobiol 24: 1-28, 2001.
21. Spejo AB, Carvalho JL, Goes AM and Oliveira AL: Neuroprotective effects of mesenchymal stem cells on spinal motoneurons following ventral root axotomy: Synapse stability and axonal regeneration. Neuroscience 250: 715-732, 2013.
22. Suzuki M, McHugh J, Tork C, Shelley B, Hayes A, Bellantuono I, Aebischer P and Svendsen CN: Direct muscle delivery of GDNF with human mesenchymal stem cells improves motor neuron survival and function in a rat model of familial ALS. Mol Ther 16: 2002-2010, 2008.
23. Rind HB, Butowt R and von Bartheld CS: Synaptic targeting of retrogradely transported trophic factors in motoneurons: Comparison of glial cell line-derived neurotrophic factor, brain-derived neurotrophic factor, and cardiotrophin-1 with tetanus toxin. J Neurosci 25: 539-549, 2005.
24. Rodrigues Hell RC, Silva Costa MM, Goes AM and Oliveira AL: Local injection of BDNF producing mesenchymal stem cells increases neuronal survival and synaptic stability following ventral root avulsion. Neurobiol Dis 33: 290-300, 2009.
25. Wong WK, Cheung AW, Yu SW, Sha O and Cho EY: Hepatocyte growth factor promotes long-term survival and axonal regeneration of retinal ganglion cells after optic nerve injury: Comparison with CNTF and BDNF. CNS Neurosci Ther 20: 916-929, 2014.
26. Difato F, Tsushima H, Pesce M, Benfenati F, Blau A and Chieregatti E: The formation of actin waves during regeneration after axonal lesion is enhanced by BDNF. Sci Rep 1: 183, 2011.
27. Haninec P, Kaiser R, Bobek V and Dubový P: Enhancement of musculocutaneous nerve reinnervation after vascular endothelial growth factor (VEGF) gene therapy. BMC Neurosci 13: 57, 2012.
28. Moimas S, Novati F, Ronchi G, Zacchigna S, Fregnan F, Zentilin L, Papa G, Giacca M, Geuna S, Perroteau I, et al: Effect of vascular endothelial growth factor gene therapy on post-traumatic peripheral nerve regeneration and denervation-related muscle atrophy. Gene Ther 20: 1014-1021, 2013.